

Supporting Information

SANS Quantification of Bound Water in Water-Soluble Polymers Across Multiple Concentration Regimes

*Helen Yao and Bradley D. Olsen**

Department of Chemical Engineering, Massachusetts Institute of Technology, Cambridge,
Massachusetts 02139, United States

*Corresponding Author

Bradley D. Olsen

TEL: (617) 715-4548

Email: bdolsen@mit.edu

Table of Contents

Polymer Gel Permeation Chromatography (GPC) Traces.....	3
Proton Nuclear Magnetic Resonance (NMR) Spectra.....	4
Overlap Concentration.....	6
Turbidimetry.....	7
Q-Q Plots.....	8
SANS Fitting.....	13
Fitting Results by Method.....	13
CV-MF-SLD.....	13
CV-FF-SLD.....	14
CV-FF- n_H	14
CV-SF-SLD.....	15
CV-SF- n_H	16
Determination of the Scattering Length Density (SLD).....	17
CV-MF-SLD.....	17
CV-FF-SLD.....	18
CV-FF- n_H	19
CV-SF-SLD.....	19
CV-SF- n_H	20
Form Factor/Structure Factor.....	22
Dilute Solution.....	22
Semidilute Solution.....	24
Concentrated Solution.....	25
Hydration Number in Dilute Solution (Change in Scale).....	27
Hypothesis Testing, Effect Size, and Box-and-whisker Plots.....	28
Hydration Number in Concentrated Solution (300 mg/mL).....	31
Estimations of Blob Correlation Length.....	32
PNIPAM Microglobule Formation.....	33
References.....	34

Polymer Gel Permeation Chromatography (GPC) Traces

Poly(*N*-isopropylacrylamide) (PNIPAM) and poly(hydroxypropyl acrylate) (HPHA) were characterized on a Waters system using two ResiPore Columns in *N,N*-dimethylformamide (DMF) with 0.02 M lithium bromide (LiBr) as the mobile phase. The dn/dc values for PNIPAM and PHPA in DMF are 0.0761¹ and 0.0533² mL g⁻¹, respectively. Poly(3-[*N*-(2-methacroyloyethyl)-*N,N*-dimethylammonio]propane sulfonate) (PDMAPS) was characterized on an Agilent Technologies 1260 Infinity system using two Aquagel columns in 0.5 M NaCl (aq) with 0.012% sodium azide as the mobile phase. The dn/dc for PDMAPS in this solvent is 0.1423 mL g⁻¹.³ All GPC traces were collected using Wyatt refractive index detectors.

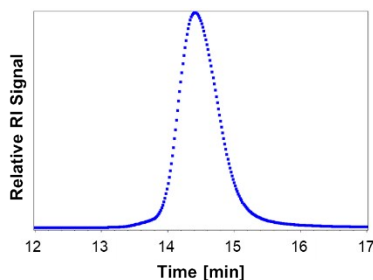


Figure S1. Relative refractive index (RI) GPC trace for purified PNIPAM with $M_n = 28,050$ Da and $\mathcal{D} = 1.03$.

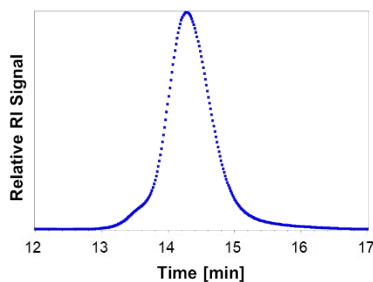


Figure S2. Relative refractive index GPC trace for purified PHPA with $M_n = 27,960$ Da and $\mathcal{D} = 1.07$.

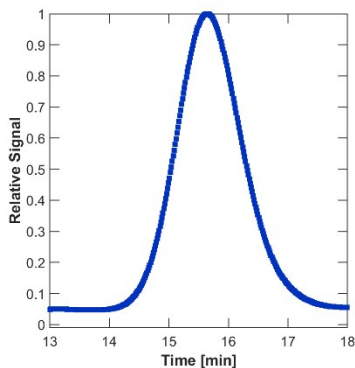


Figure S3. Relative refractive index GPC trace for purified PDMAPS with $M_n = 32,500$ Da and $\mathcal{D} = 1.18$.

Proton Nuclear Magnetic Resonance (NMR) Spectra

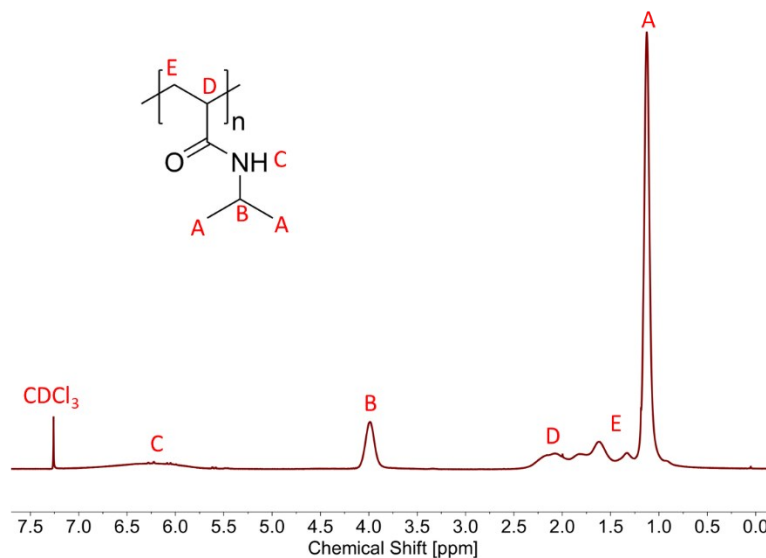


Figure S4. ¹H NMR spectrum for PNIPAM. Peaks are indexed as follows (in ppm): $\delta_A = 1.13$, $\delta_B = 3.99$, $\delta_C = 6.22$, $\delta_D = 2.08$, and $\delta_E = 1.33$. The peaks were referenced to the solvent peak at 7.26 ppm (CDCl₃). There are no additional peaks above the range shown here.

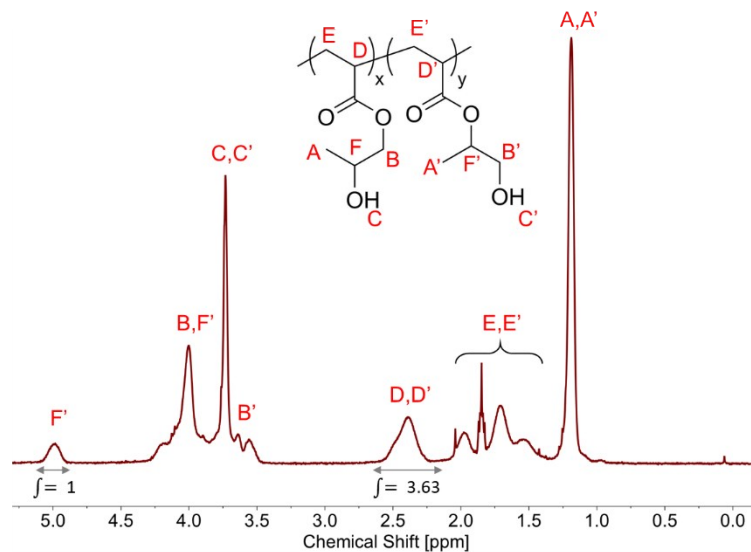


Figure S5. ¹H NMR spectrum for PHPA. Peaks are indexed as follows (in ppm): $\delta_{A,A'} = 1.19$; $\delta_B = 4.00$; $\delta_{B'} = 3.62, 3.64$; $\delta_{C,C'} = 3.73$; $\delta_{D,D'} = 2.39$; $\delta_{E,E'} = 1.53, 1.71, 1.85, 1.97$; $\delta_F = 4.00$, and $\delta_{F'} = 4.98$. The peaks were referenced to the solvent peak at 7.26 ppm (CDCl_3 , not shown). There are no additional peaks above the range shown here, besides the solvent peak at CDCl_3 . To approximate the fraction of each monomer, the following ratio was used:

$$\frac{\int_{F'} F'}{\int_{D,D'}} = \frac{y}{x+y} = \frac{1}{3.63} = 0.275$$

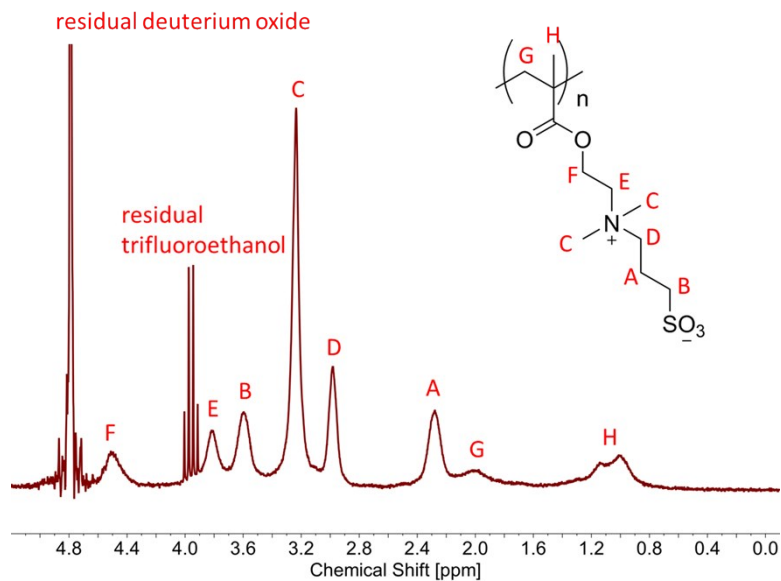


Figure S6. ¹H NMR spectrum for PDMAPS used in this thesis. Peaks are indexed as follows (in ppm): $\delta_A = 2.28$, $\delta_B = 3.60$, $\delta_C = 3.23$, $\delta_D = 2.98$, $\delta_E = 3.81$, $\delta_F = 4.50$, $\delta_G = 1.99$, and $\delta_H = 1.00-1.14$. The peaks were referenced to the solvent peak at 4.79 (D₂O). The quartet at 3.97 ppm can be indexed to residual trifluoroethanol.

Overlap Concentration

The overlap concentration was calculated to determine the location of the boundary between dilute and semidilute solutions. The overlap volume fraction was estimated for PNIPAM, PHPA, and PDMAAPS using Equation S1:⁴

$$\phi^* = \frac{\text{molecular volume of polymer}}{\text{volume of polymer coil}} = \frac{M}{N_A \rho v_{coil}} \quad (\text{S1})$$

Here, M is the molar mass of the polymer, N_A is Avogadro's number, ρ is the polymer density, and v_{coil} is the volume of the polymer coil, which can be estimated as the cube of the end-to-end distance $\langle r^2 \rangle^{1/2}$. The end-to-end distance was estimated from radius of gyration, $\langle r^2 \rangle^{1/2} = \frac{1}{6} R_g^2$, where R_g was taken from the D-FF-SLD method (Table 3), i.e. a dilute solution SANS experiment.

Turbidimetry

Turbidimetry was measured by UV-Vis absorbance using a 1 cm path length quartz cuvette in a Varian Cary 50 UV-Vis spectrometer. Polymer solutions for PNIPAM, PHPA, and PDMAPS were prepared at 13.75, 50, 250, and 300 mg/mL in filtered Milli-Q water, which were the same concentrations measured for SANS experiments. Reversibility was determined using heating and cooling ramps. For higher concentration samples, a stir bar was used to break up large polymer agglomerates formed after macrophase separation. Each measurement was corrected for a Milli-Q water background and a blocked beam background. For all polymers, the temperature was set to the initial point and held for 5 minutes for equilibration. This was followed by a 1 °C/min ramp to a second set point, with temperature readings collected every 6 seconds in 0.1 °C intervals. At the second set point, the sample was held for 5 minutes with data collection. The temperature was then ramped back to the first set point at 1 °C/min, collecting at the same frequency as the first ramp. Once back at the first set point, the temperature was held for 5 minutes, after which the measurement was terminated. For lower critical solution temperature (LCST) polymers, the first set point is a low temperature below the LCST, and the second one is a higher temperature above the LCST. For upper critical solution temperature (UCST) polymers, the first set point is a high temperature above the UCST, and the second is a lower temperature below the UCST before ramping up again.

A MATLAB script was used to convert absorbance to transmittance by Equation S2. Transmittance (T) was calculated by Equation S2, where A is the absorbance and 2 is the maximum absorbance.

$$T = 10^{2-A} \quad (\text{S2})$$

Transmission was calculated by normalizing the raw transmittance to the maximum range of the transmittance measurements. The cloud point temperature was defined as the temperature at which 50% of the normalized transmission was lost. For each heating and cooling ramp, a cloud point temperature was calculated except in cases where the macrophase separation could not be reversed by the stir bar on the time scale of the experiment. Cloud point curves are shown in Figure S7.

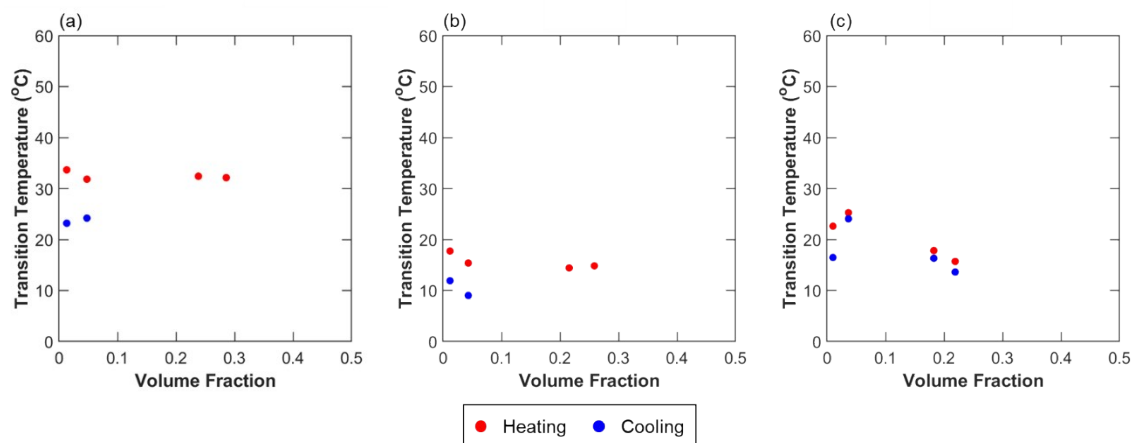


Figure S7. Cloud point curves for (a) PNIPAM, (b) PHPA, and (c) PDMAPS. PNIPAM and PHPA are LCST polymers, and PDMAPS is an UCST polymer.

Q-Q Plots

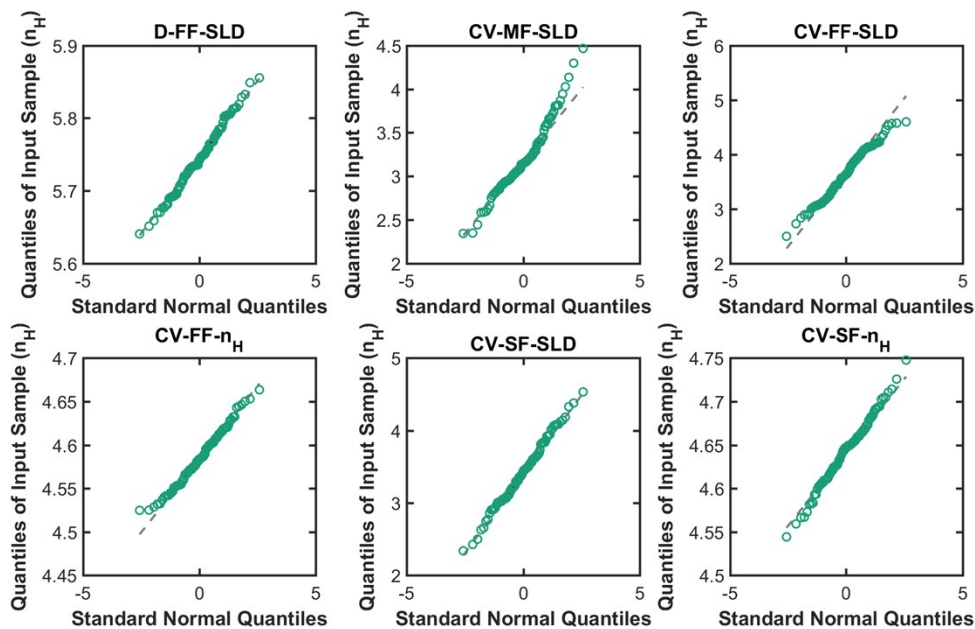


Figure S8. Q-Q plots for hydration number obtained from each fitting method for PNIPAM at a concentration of 13.75 mg/mL

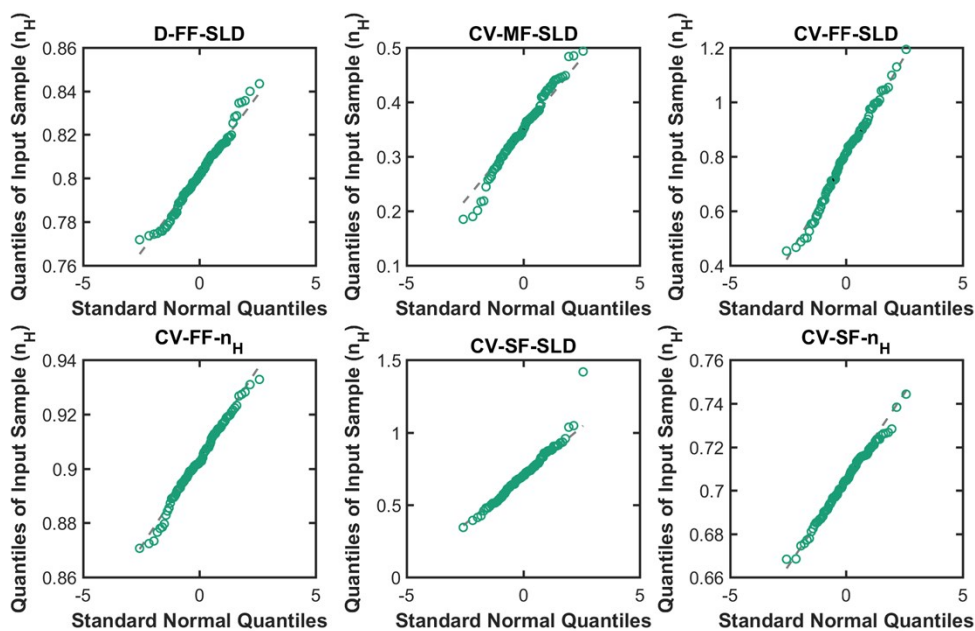


Figure S9. Q-Q plots for hydration number obtained from each fitting method for PHPA at a concentration of 13.75 mg/mL

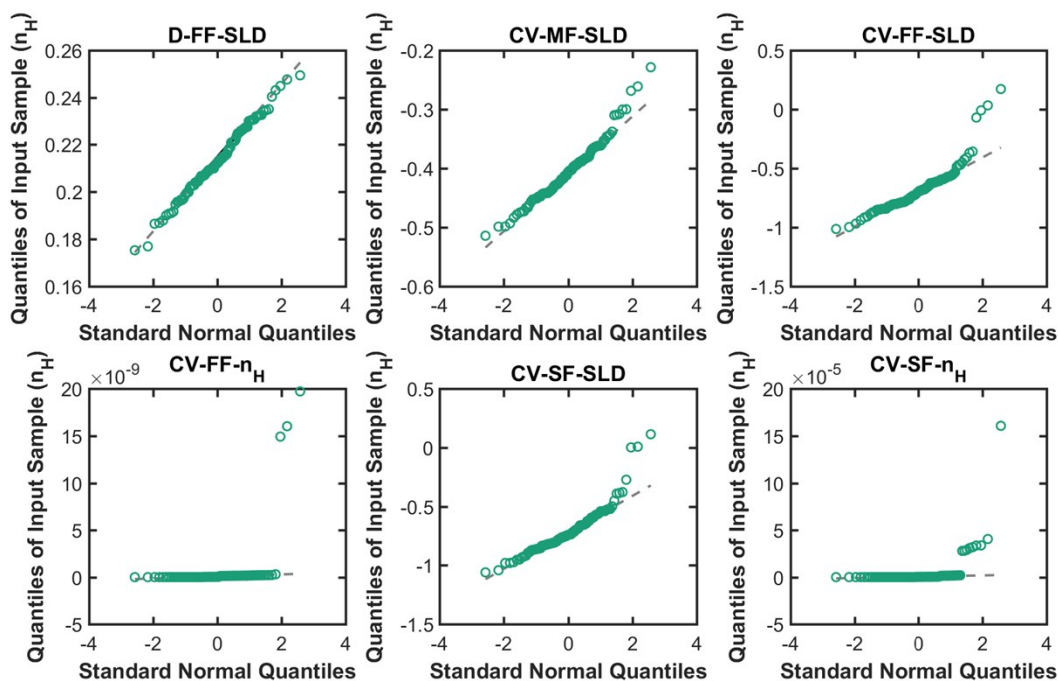


Figure S10. Q-Q plots for hydration number obtained from each fitting method for PDMAPS at a concentration of 13.75 mg/mL

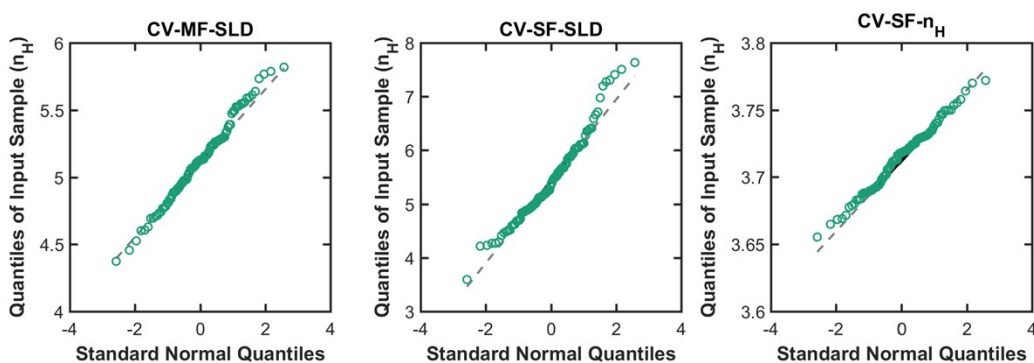


Figure S11. Q-Q plots for hydration number obtained from each fitting method for PNIPAM at a concentration of 50 mg/mL

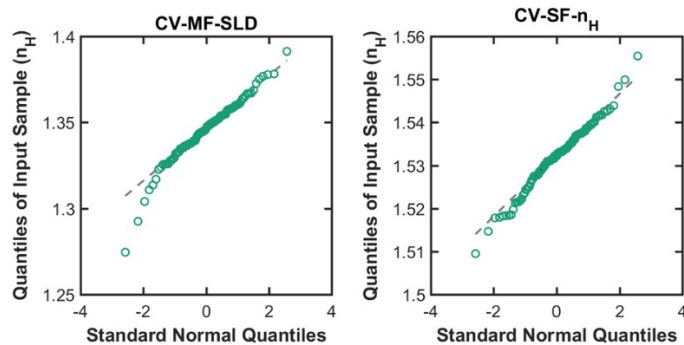


Figure S12. Q-Q plots for hydration number obtained from each fitting method for PHPA at a concentration of 50 mg/mL

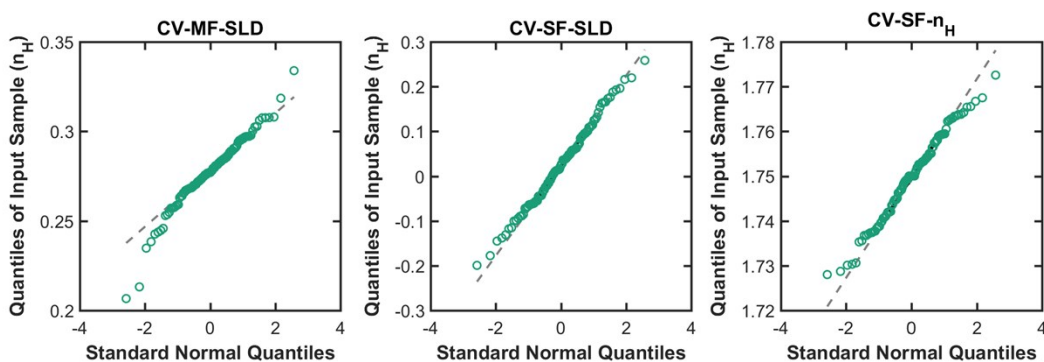


Figure S13. Q-Q plots for hydration number obtained from each fitting method for PDMAPS at a concentration of 50 mg/mL

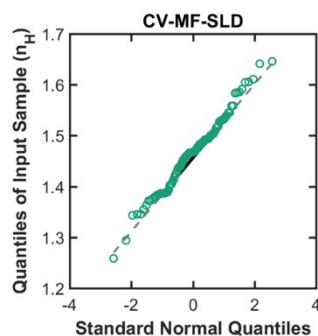


Figure S14. Q-Q plot for hydration number obtained from the CV-MF-SLD method for PNIPAM at a concentration of 250 mg/mL. The other methods were incompatible with the PNIPAM structure factor.

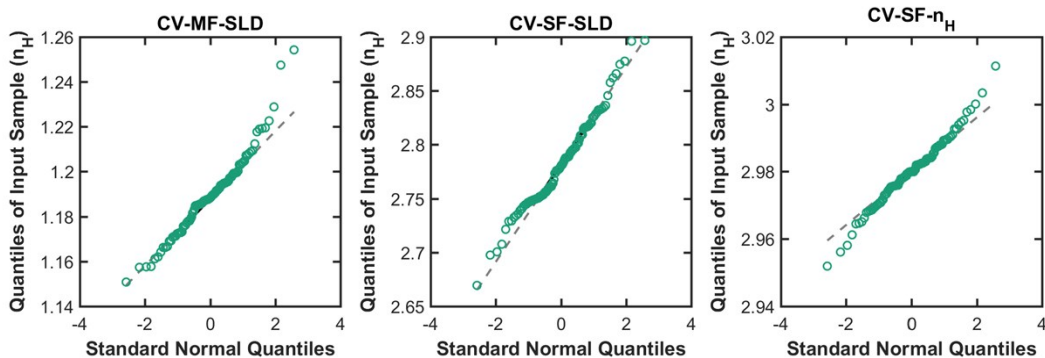


Figure S15. Q-Q plot for hydration number obtained from each fitting method for PHPA at a concentration of 250 mg/mL.

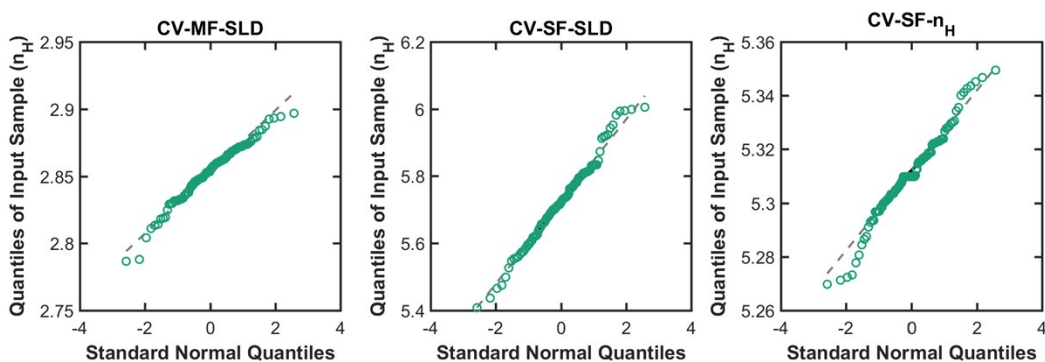


Figure S16. Q-Q plot for hydration number obtained from each fitting method for PDMAPS at a concentration of 250 mg/mL.

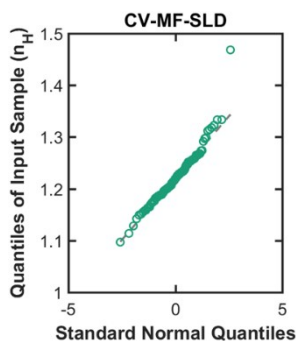


Figure S17. Q-Q plot for hydration number obtained from the CV-MF-SLD method for PNIPAM at a concentration of 300 mg/mL. The other methods were incompatible with the PNIPAM structure factor.

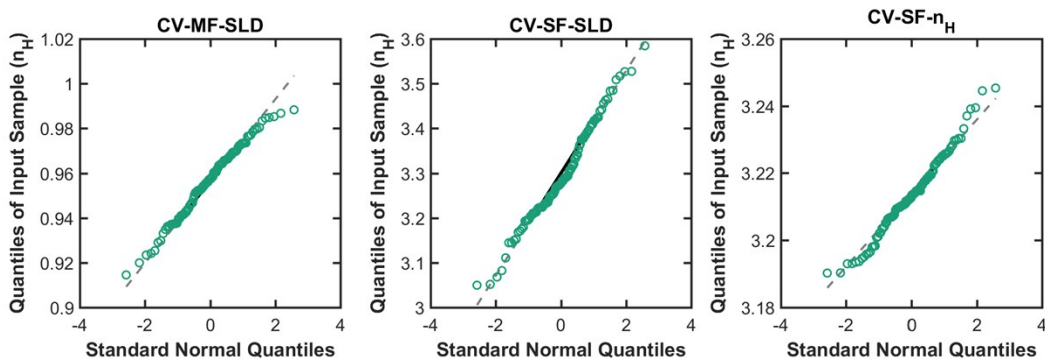


Figure S18. Q-Q plot for hydration number obtained from each fitting method for PHPA at a concentration of 300 mg/mL.

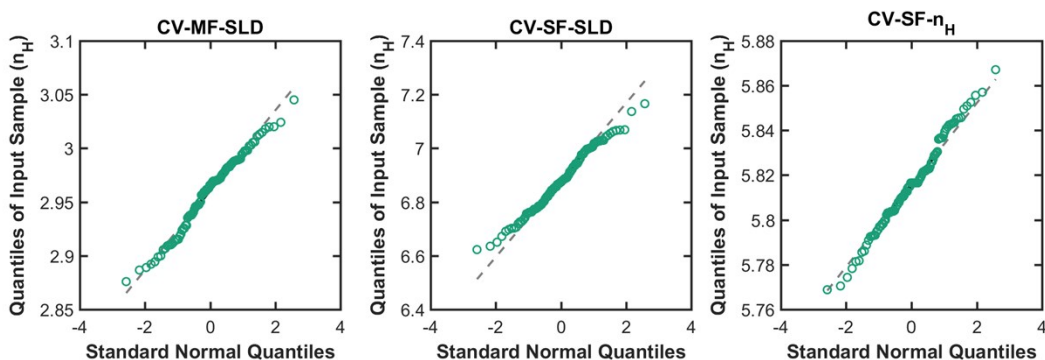


Figure S19. Q-Q plot for hydration number obtained from each fitting method for PDMAPS at a concentration of 300 mg/mL.

SANS Fitting

Fitting Results by Method

The D-FF-SLD method is already shown in the main manuscript (Figure 2).

CV-MF-SLD

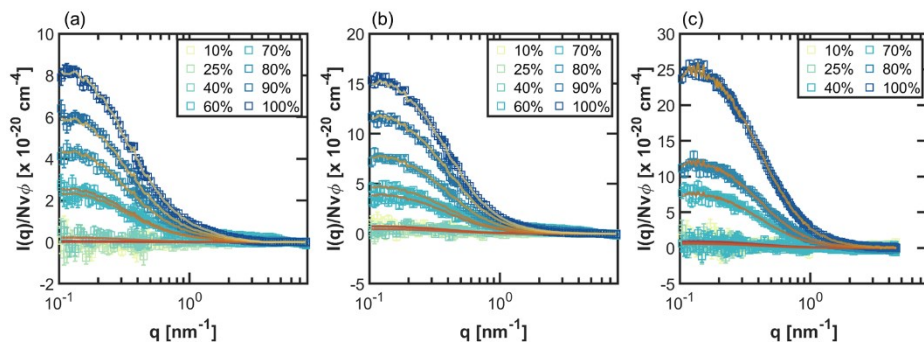


Figure S20. SANS fitting through CV-MF-SLD for (a) PNIPAM, (b) PHPA, and (c) PDMAPS at 13.75 mg/mL

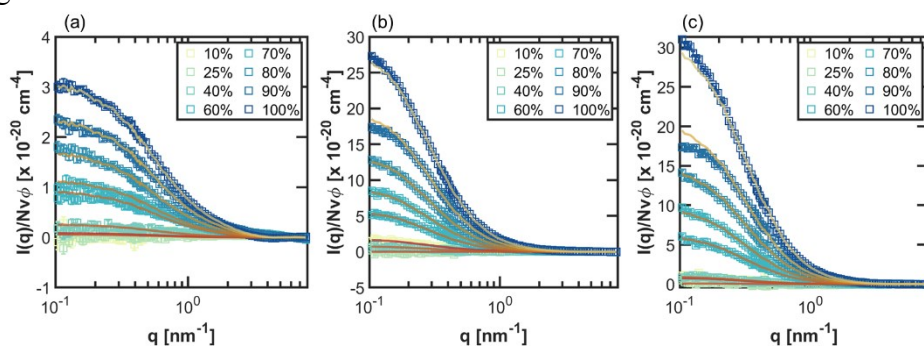


Figure S21. SANS fitting through CV-MF-SLD for (a) PNIPAM, (b) PHPA, and (c) PDMAPS at 50 mg/mL

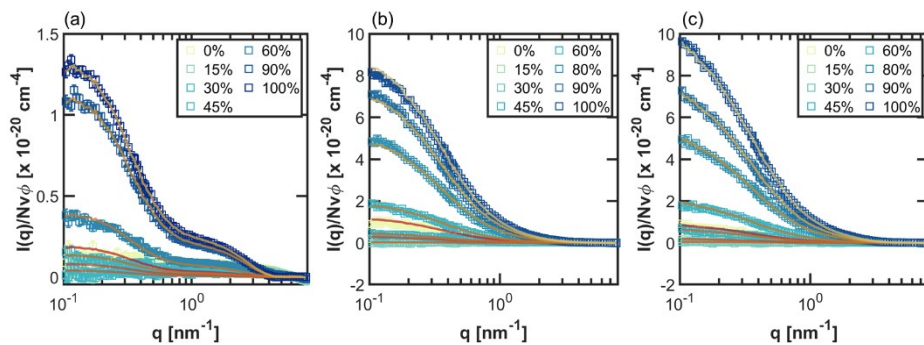


Figure S22. SANS fitting through CV-MF-SLD for (a) PNIPAM, (b) PHPA, and (c) PDMAPS at 250 mg/mL

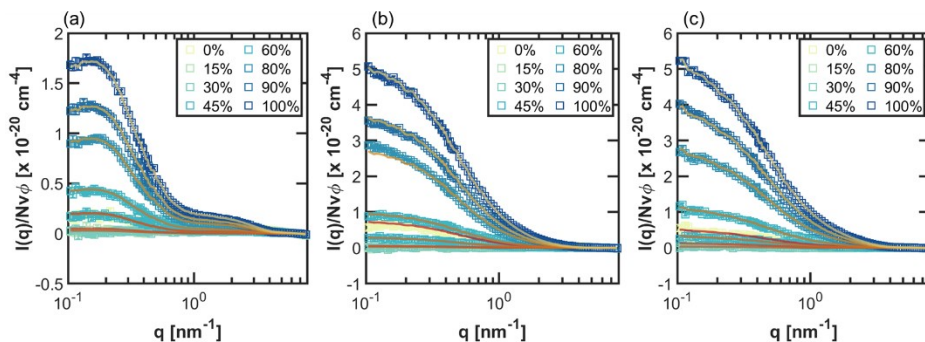


Figure S23. SANS fitting through CV-MF-SLD for (a) PNIPAM, (b) PHPA, and (c) PDMAPS at 300 mg/mL

CV-FF-SLD

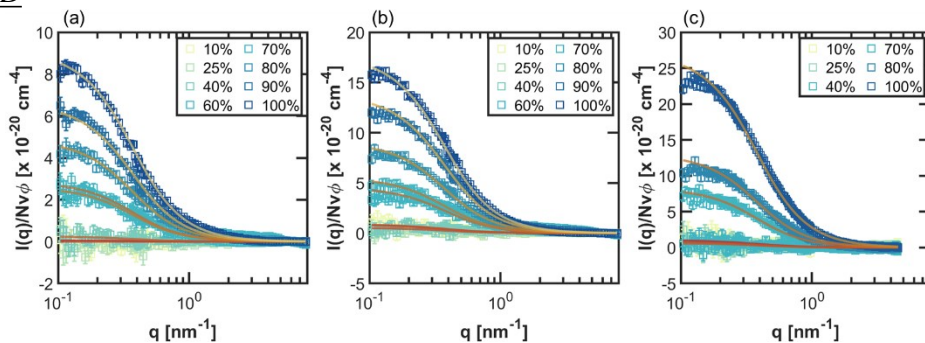


Figure S24. SANS fitting through CV-FF-SLD for (a) PNIPAM, (b) PHPA, and (c) PDMAPS at 13.75 mg/mL

CV-FF-n_H

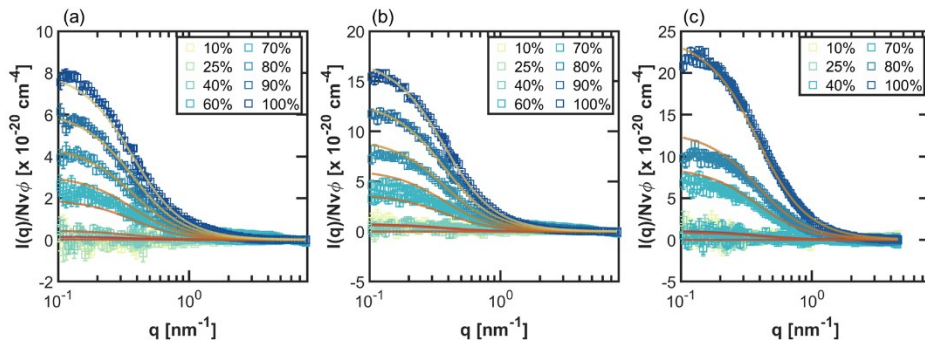


Figure S25. SANS fitting through CV-FF-n_H for (a) PNIPAM, (b) PHPA, and (c) PDMAPS at 13.75 mg/mL

CV-SF-SLD

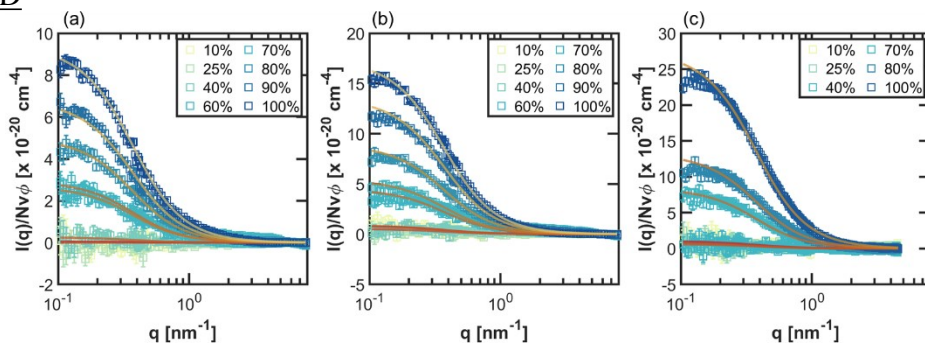


Figure S26. SANS fitting through CV-SF-SLD for (a) PNIPAM, (b) PHPA, and (c) PDMAPS at 13.75 mg/mL

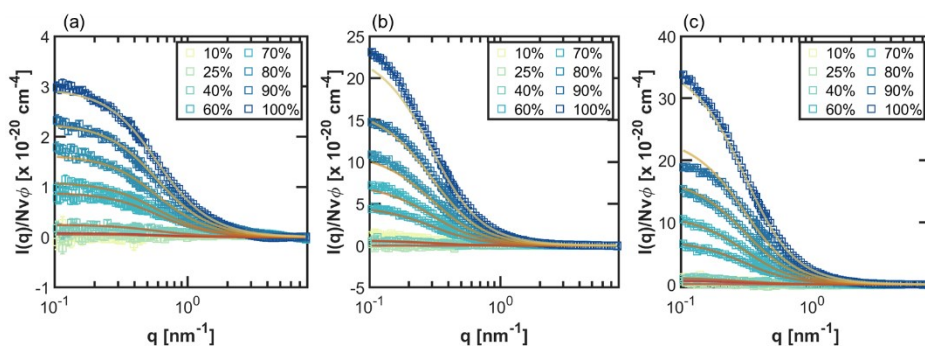


Figure S27. SANS fitting through CV-SF-SLD for (a) PNIPAM, (b) PHPA, and (c) PDMAPS at 50 mg/mL

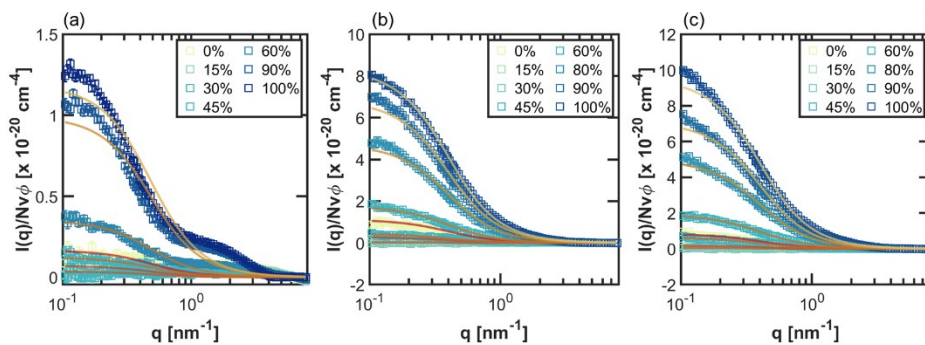


Figure S28. SANS fitting through CV-SF-SLD for (a) PNIPAM, (b) PHPA, and (c) PDMAPS at 250 mg/mL

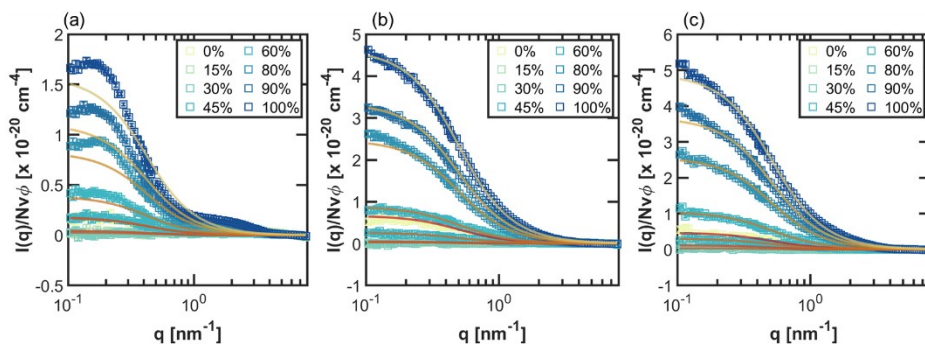


Figure S29. SANS fitting through CV-SF-SLD for (a) PNIPAM, (b) PHPA, and (c) PDMAPS at 300 mg/mL

CV-SF-n_H

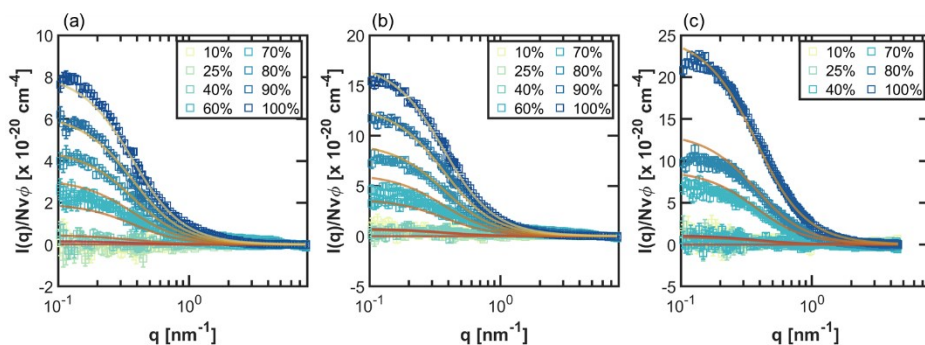


Figure S30. SANS fitting through CV-SF-n_H for (a) PNIPAM, (b) PHPA, and (c) PDMAPS at 13.75 mg/mL

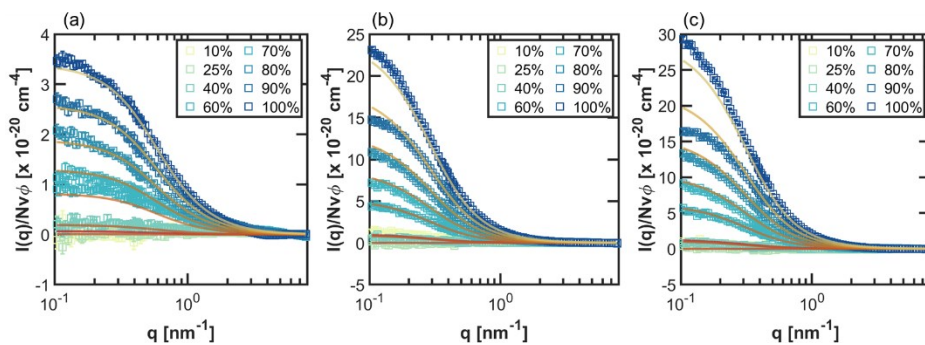


Figure S31. SANS fitting through CV-SF-n_H for (a) PNIPAM, (b) PHPA, and (c) PDMAPS at 50 mg/mL

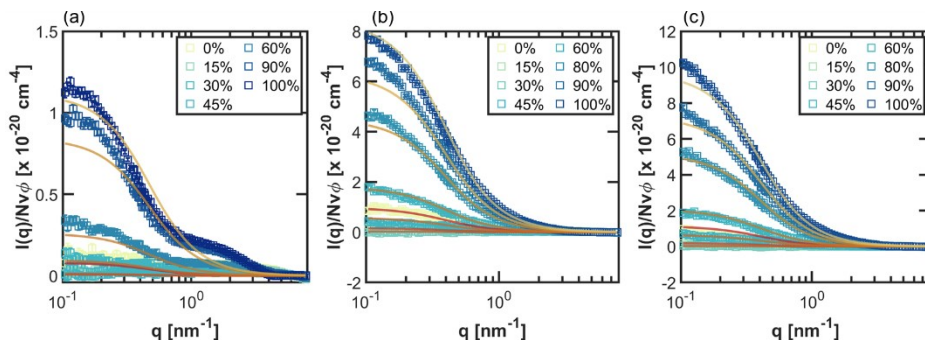


Figure S32. SANS fitting through CV-SF- n_H for (a) PNIPAM, (b) PHPA, and (c) PDMAPS at 250 mg/mL

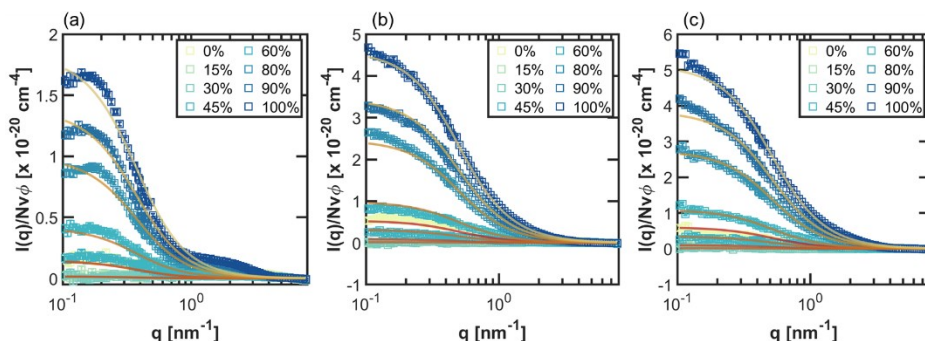


Figure S33. SANS fitting through CV-SF- n_H for (a) PNIPAM, (b) PHPA, and (c) PDMAPS at 300 mg/mL

Determination of the Scattering Length Density (SLD)

In D-FF-SLD, only the SLD for 100% D_2O solutions is determined. For contrast matching, the difference in SLD of solvent and polymer is fit to a quadratic function of f , the fraction of D_2O in the blend. The resulting SLDs are shown in the following figures.

CV-MF-SLD

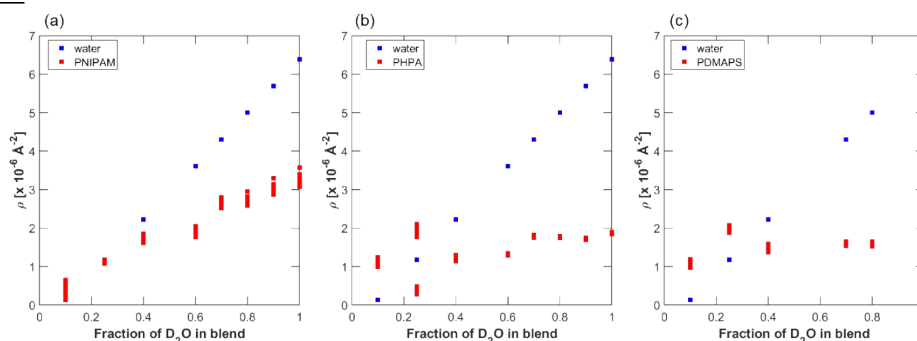


Figure S34. SLD of polymer determined through CV-MF-SLD for (a) PNIPAM, (b) PHPA, and (c) PDMAPS at 13.75 mg/mL

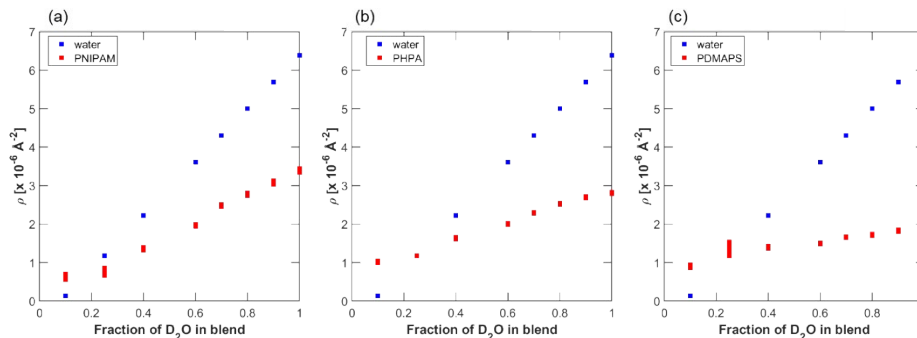


Figure S35. SLD of polymer determined through CV-MF-SLD for (a) PNIPAM, (b) PHPA, and (c) PDMAPS at 50 mg/mL

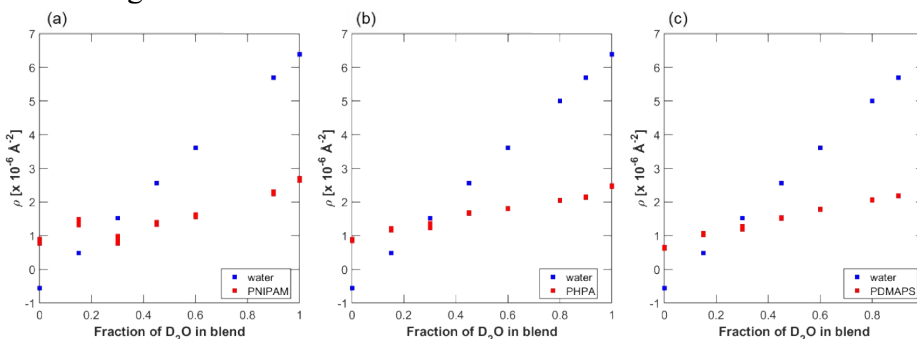


Figure S36. SLD of polymer determined through CV-MF-SLD for (a) PNIPAM, (b) PHPA, and (c) PDMAPS at 250 mg/mL

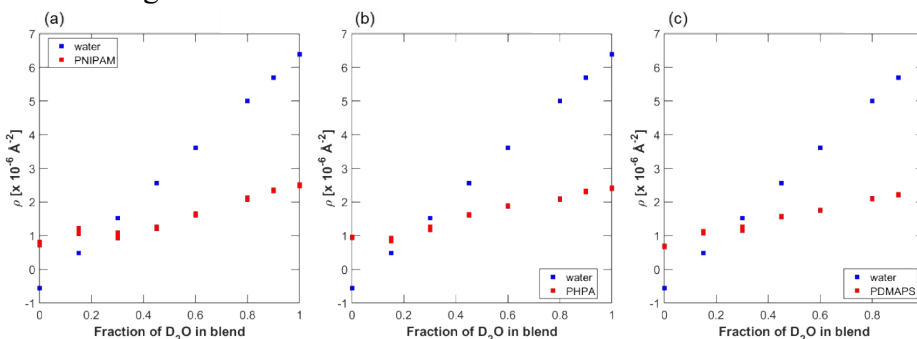


Figure S37. SLD of polymer determined through CV-MF-SLD for (a) PNIPAM, (b) PHPA, and (c) PDMAPS at 300 mg/mL

CV-FF-SLD

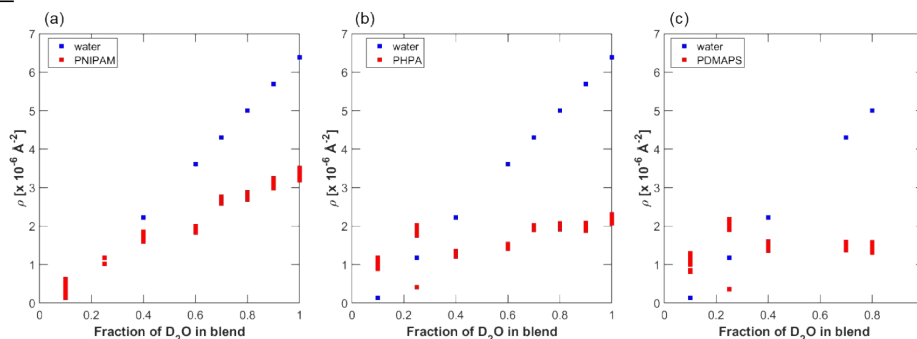


Figure S38. SLD of polymer determined through CV-FF-SLD for (a) PNIPAM, (b) PHPA, and (c) PDMAPS at 13.75 mg/mL

CV-FF-n_H

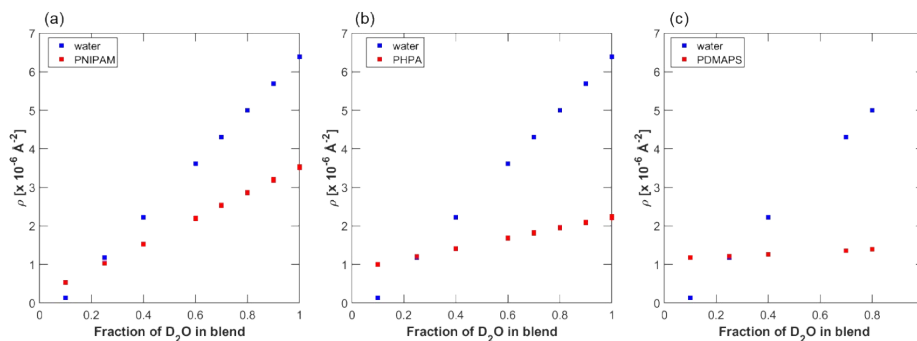


Figure S39. SLD of polymer determined through CV-FF-n_H for (a) PNIPAM, (b) PHPA, and (c) PDMAPS at 13.75 mg/mL

CV-SF-SLD

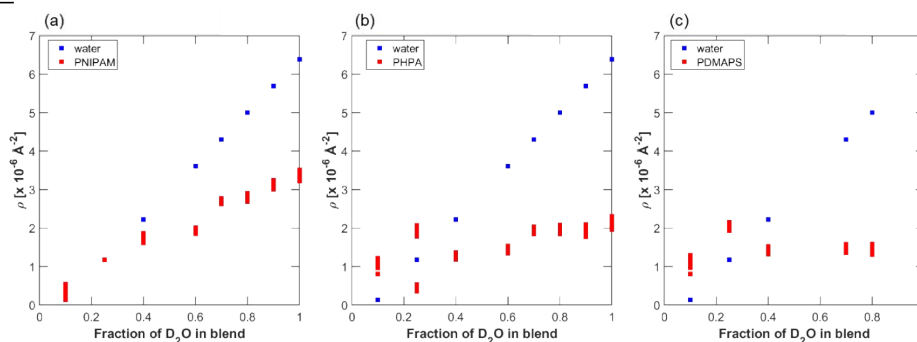


Figure S40. SLD of polymer determined through CV-SF-SLD for (a) PNIPAM, (b) PHPA, and (c) PDMAPS at 13.75 mg/mL

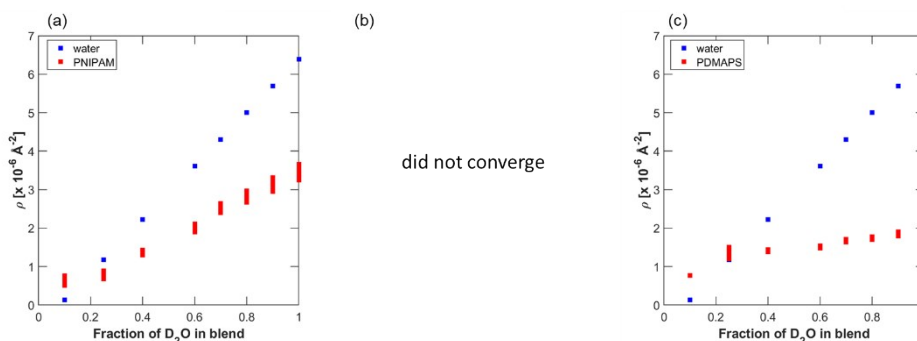


Figure S41. SLD of polymer determined through CV-SF-SLD for (a) PNIPAM, (b) PHPA, and (c) PDMAPS at 50 mg/mL

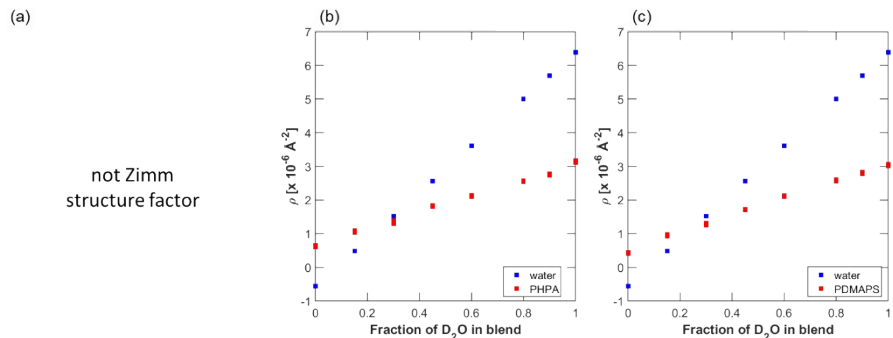


Figure S42. SLD of polymer determined through CV-SF-SLD for (a) PNIPAM, (b) PHPA, and (c) PDMAPS at 250 mg/mL

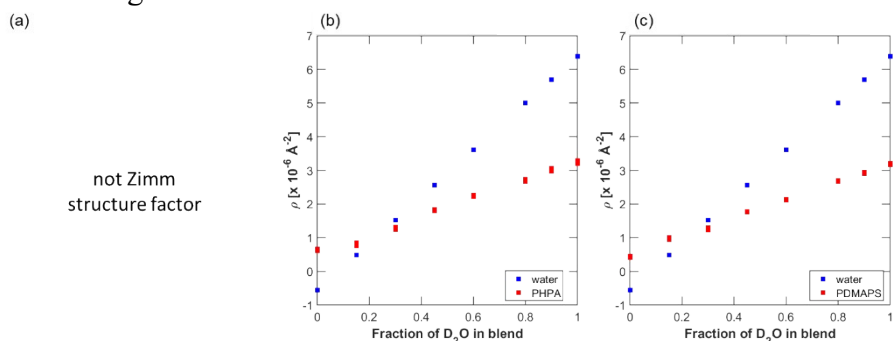


Figure S43. SLD of polymer determined through CV-SF-SLD for (a) PNIPAM, (b) PHPA, and (c) PDMAPS at 300 mg/mL

CV-SF- n_H

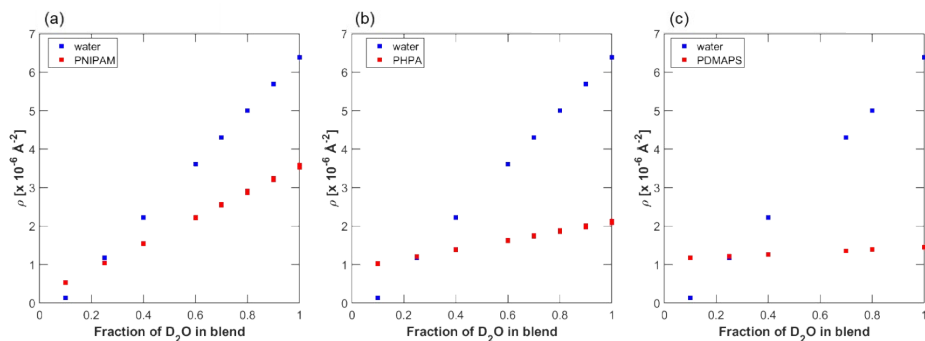


Figure S44. SLD of polymer determined through CV-SF- n_H for (a) PNIPAM, (b) PHPA, and (c) PDMAPS at 13.75 mg/mL

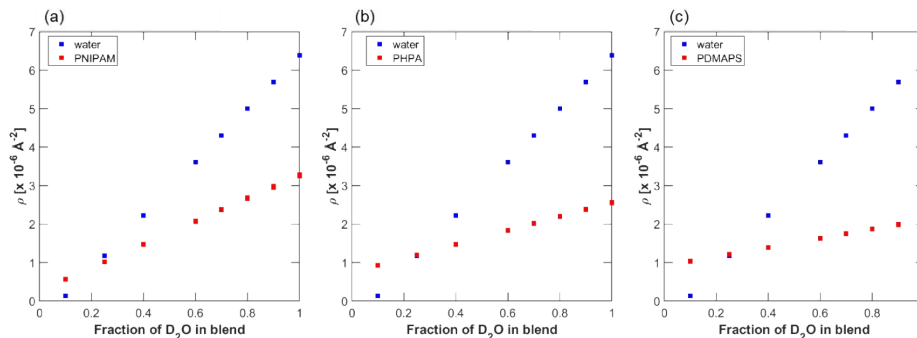


Figure S45. SLD of polymer determined through CV-SF- n_H for (a) PNIPAM, (b) PHPA, and (c) PDMAPS at 50 mg/mL

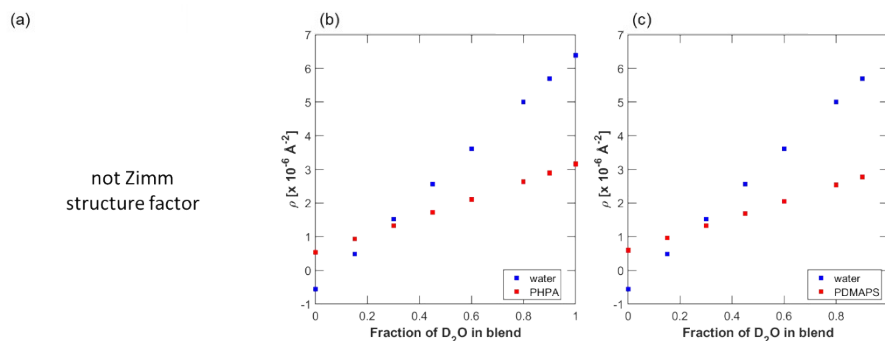


Figure S46. SLD of polymer determined through CV-SF- n_H for (a) PNIPAM, (b) PHPA, and (c) PDMAPS at 250 mg/mL

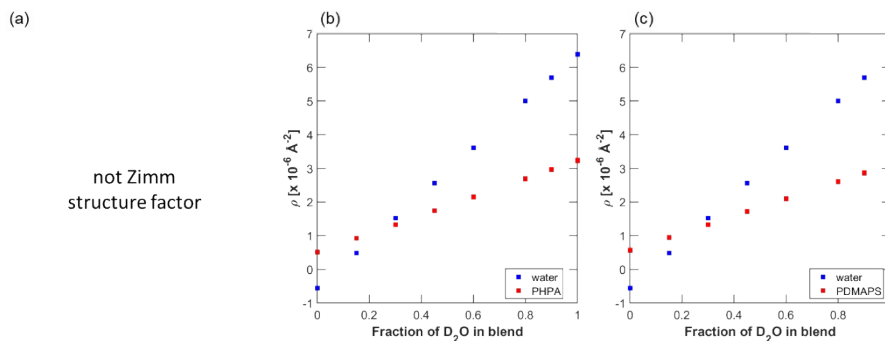


Figure S47. SLD of polymer determined through CV-SF- n_H for (a) PNIPAM, (b) PHPA, and (c) PDMAPS at 300 mg/mL

Form Factor/Structure Factor

For all figures in this section, $P(q)$ is the form factor and $G(q)$ is the generalized notation for either a form factor or a function comprising of both the structure factor and form factor. The black dotted line is only plotted for dilute solution data, as it represents the Debye form factor obtained from the D-FF-SLD method fit to the original experimental data taken in 100% D_2O . The colored lines represent form or structure factors from all bootstrapped replicates. For all methods other than D-FF-SLD, the bootstrapped replicates may deviate from the black dotted line because they use all CV-SANS blend data instead of the 100% D_2O data alone.

Dilute Solution

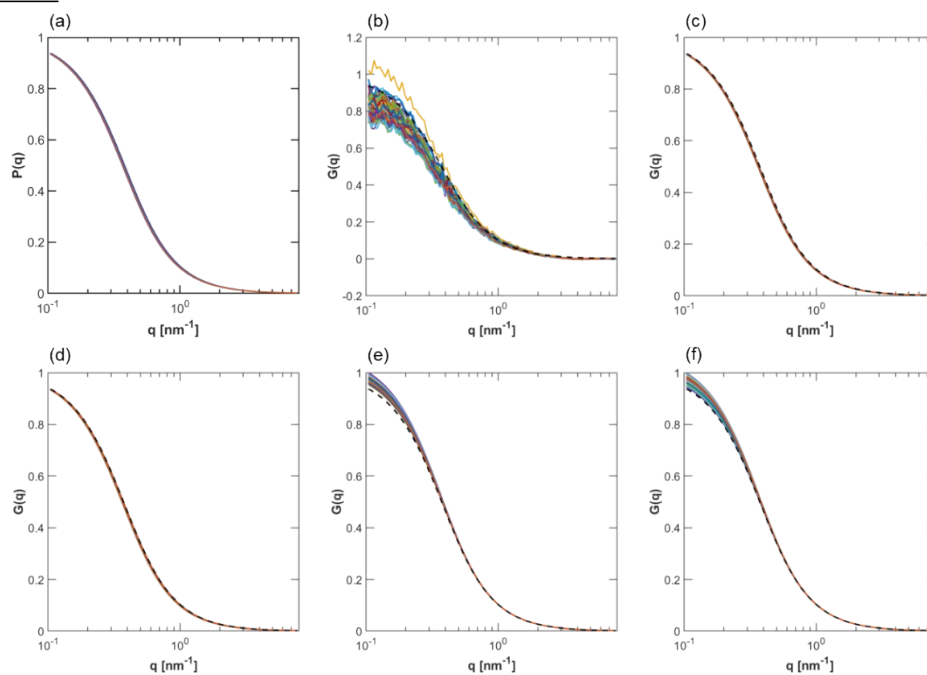


Figure S48. Form factor of PNIPAM in 13.75 mg/mL solution determined through (a) D-FF-SLD, (b) CV-MF-SLD, (c) CV-FF-SLD, (d) CV-FF- n_H , (e) CV-SF-SLD and (f) CV-SF- n_H .

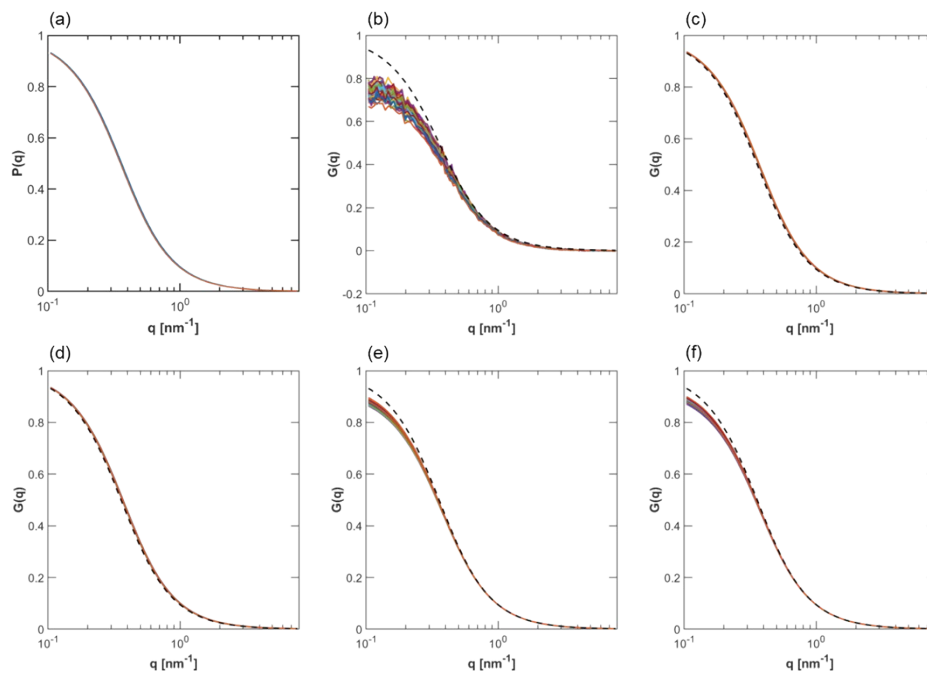


Figure S49. Form factor of PHPA in 13.75 mg/mL solution determined through (a) D-FF-SLD, (b) CV-MF-SLD, (c) CV-FF-SLD, (d) CV-FF- n_H , (e) CV-SF-SLD and (f) CV-SF- n_H .

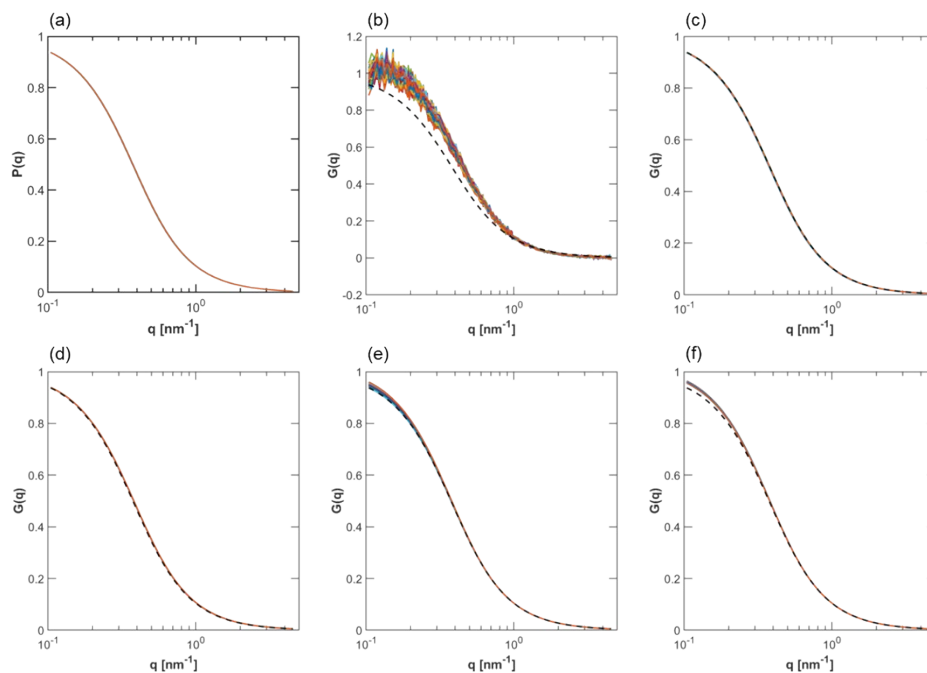


Figure S50. Form factor of PDMAPS in 13.75 mg/mL solution determined through (a) D-FF-SLD, (b) CV-MF-SLD, (c) CV-FF-SLD, (d) CV-FF- n_H , (e) CV-SF-SLD and (f) CV-SF- n_H .

Semidilute Solution

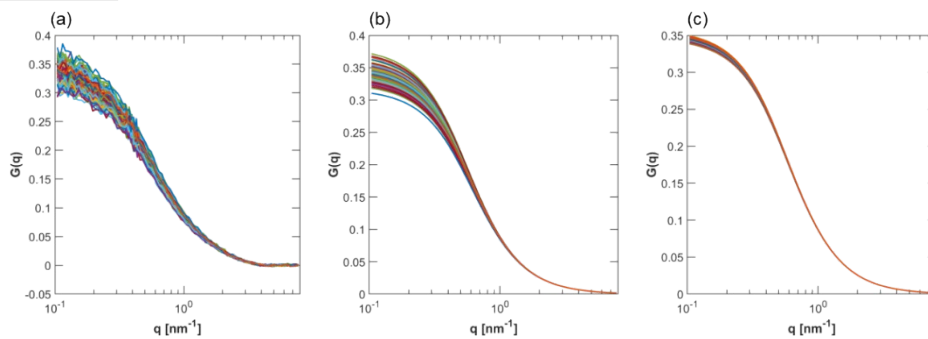


Figure S51. Structure factor of PNIPAM in 50 mg/mL solution determined through (a) CV-MF-SLD, (b) CV-SF-SLD, and (c) CV-SF- n_H

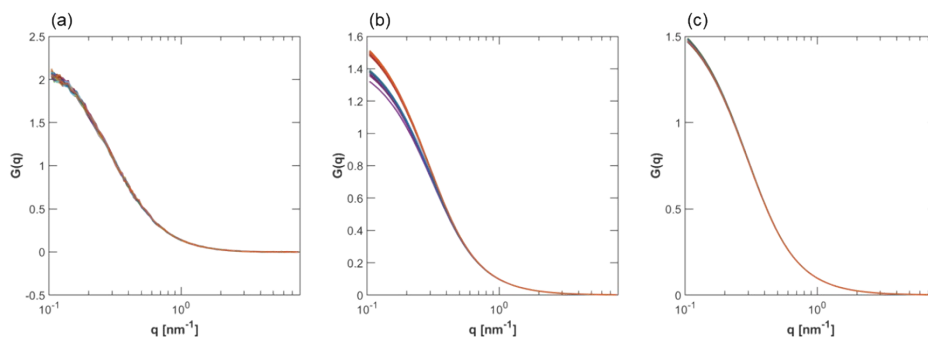


Figure S52. Structure factor of PHPA in 50 mg/mL solution determined through (a) CV-MF-SLD, (b) CV-SF-SLD, and (c) CV-SF- n_H

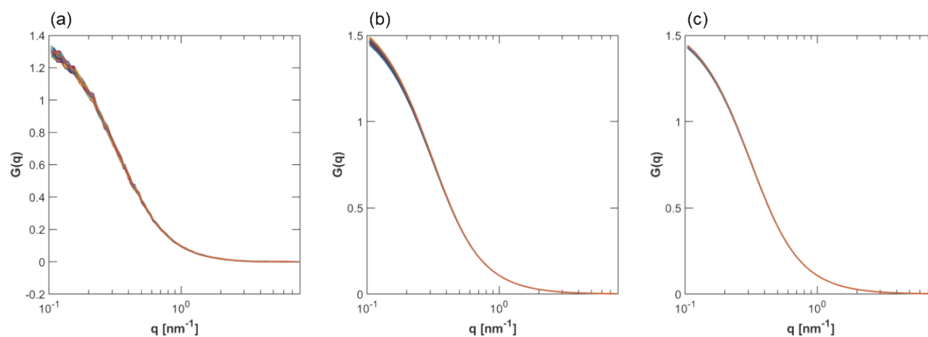


Figure S53. Structure factor of PDMAPS in 50 mg/mL solution determined through (a) CV-MF-SLD, (b) CV-SF-SLD, and (c) CV-SF- n_H

Concentrated Solution

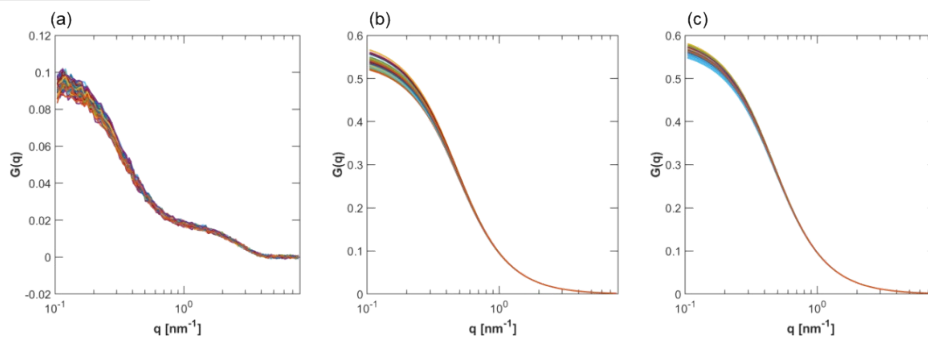


Figure S54. Structure factor of PNIPAM in 250 mg/mL solution determined through (a) CV-MF-SLD, (b) CV-SF-SLD, and (c) CV-SF- n_H

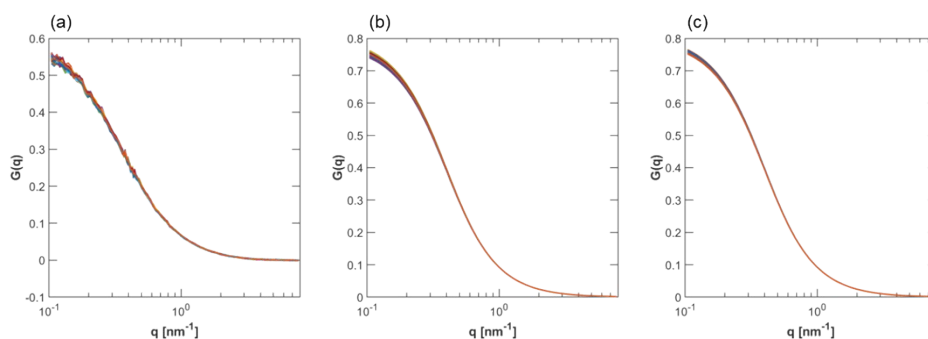


Figure S55. Structure factor of PHPA in 250 mg/mL solution determined through (a) CV-MF-SLD, (b) CV-SF-SLD, and (c) CV-SF- n_H

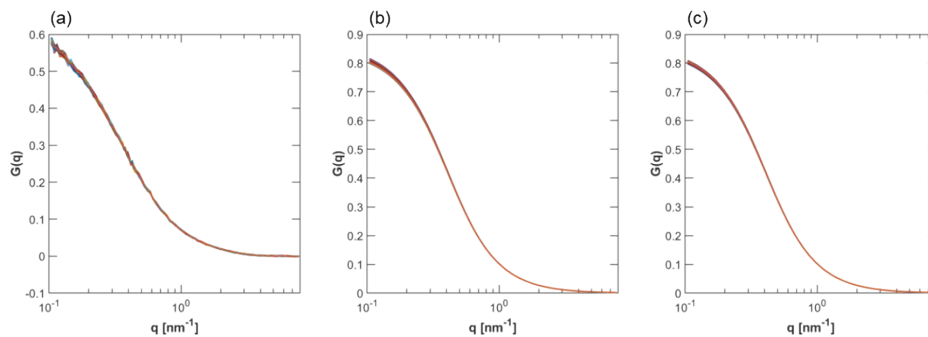


Figure S56. Structure factor of PDMAPS in 250 mg/mL solution determined through (a) CV-MF-SLD, (b) CV-SF-SLD, and (c) CV-SF- n_H

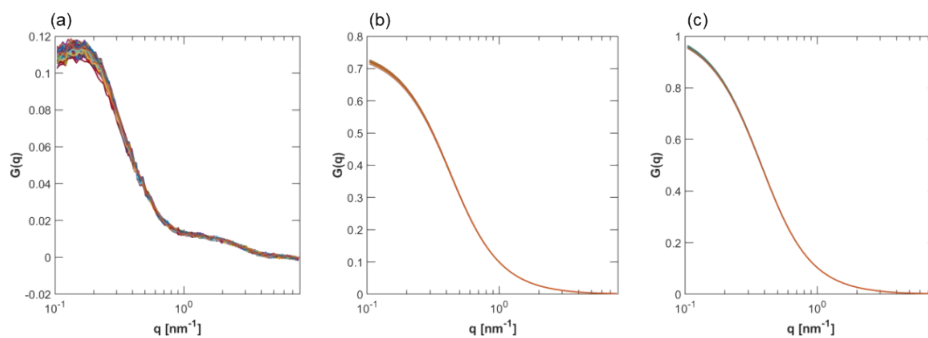


Figure S57. Structure factor of PNIPAM in 300 mg/mL solution determined through (a) CV-MF-SLD, (b) CV-SF-SLD, and (c) CV-SF- n_H

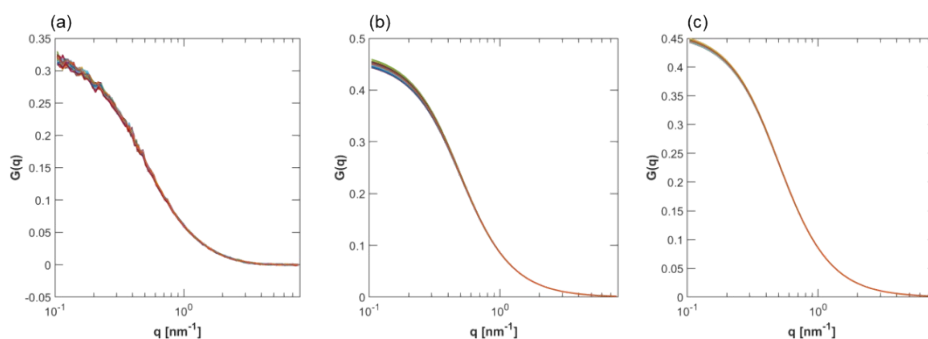


Figure S58. Structure factor of PHPA in 300 mg/mL solution determined through (a) CV-MF-SLD, (b) CV-SF-SLD, and (c) CV-SF- n_H

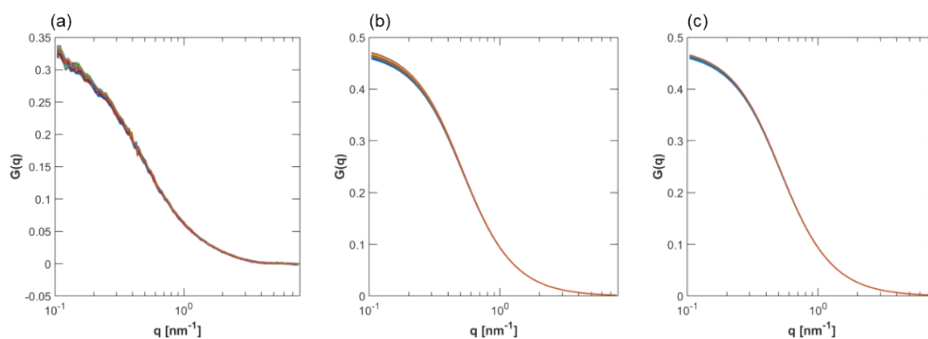


Figure S59. Structure factor of PDMAPS in 300 mg/mL solution determined through (a) CV-MF-SLD, (b) CV-SF-SLD, and (c) CV-SF- n_H

Hydration Number in Dilute Solution (Change in Scale)

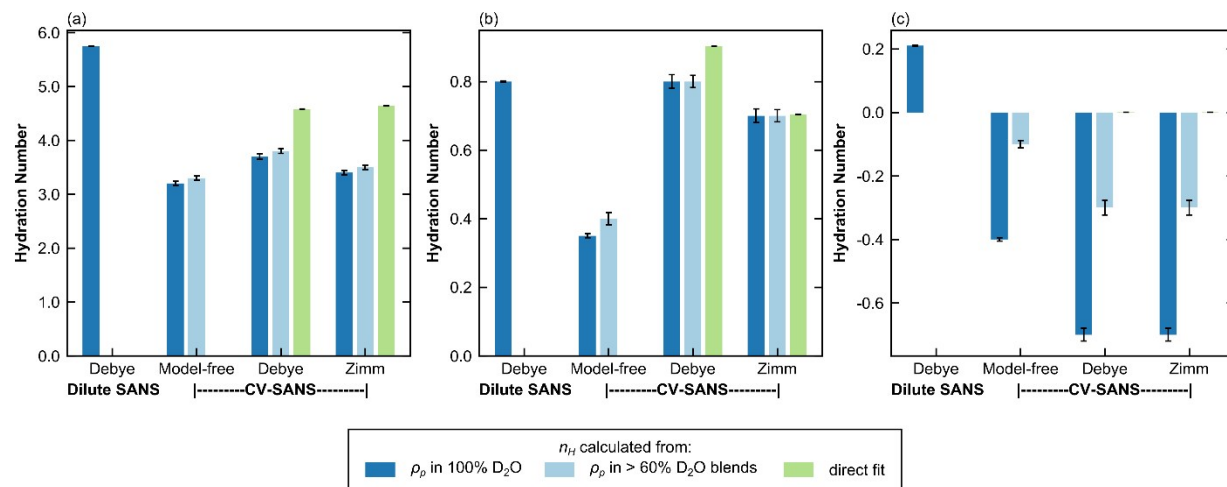


Figure S60. Bar charts comparing the hydration number obtained through different fitting methods for (a) PNIPAM, (b) PHPA, and (c) PDMAPS in dilute solution (13.75 mg/mL). The light blue bars represent hydration numbers averaged across high D₂O blends. For PDMAPS, the n_H direct fits yield a hydration number of 0 with very small error bars. Error bars represent standard error of the mean from 100 replicas.

Hypothesis Testing, Effect Size, and Box-and-whisker Plots

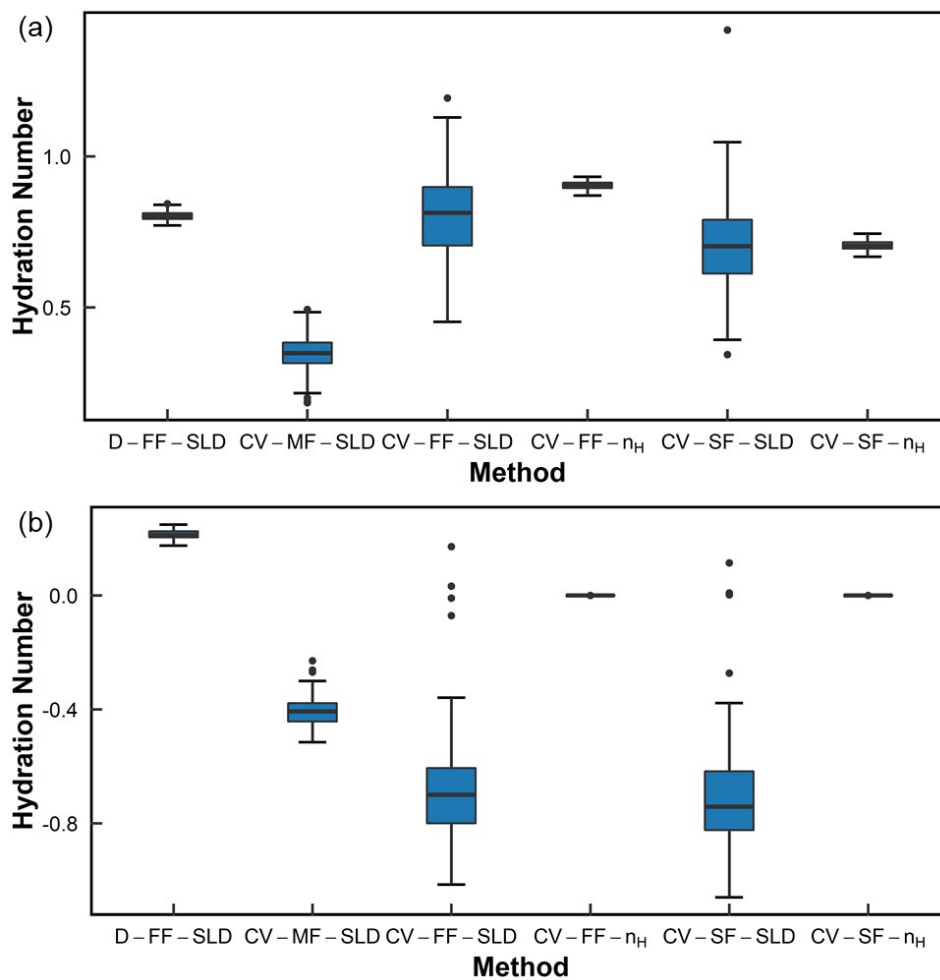


Figure S61. Box-and-whisker plots for hydration number obtained through different fitting methods for (a) PHPA and (b) PDMAPS in dilute solution (13.75 mg/mL). Each dataset is generated from 100 bootstrapped replicates.

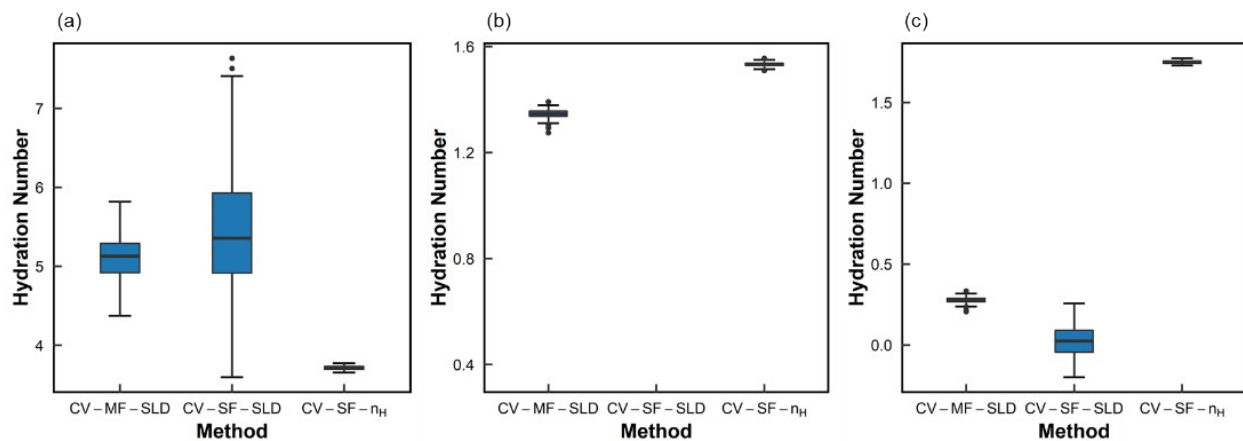


Figure S62. Box-and-whisker plots for hydration number obtained through different fitting methods for (a) PNIPAM, (b) PHPA, and (c) PDMAPS in semidilute solution (50 mg/mL). CV-SF-SLD did not converge for PHPA. Each dataset is generated from 100 bootstrapped replicates.

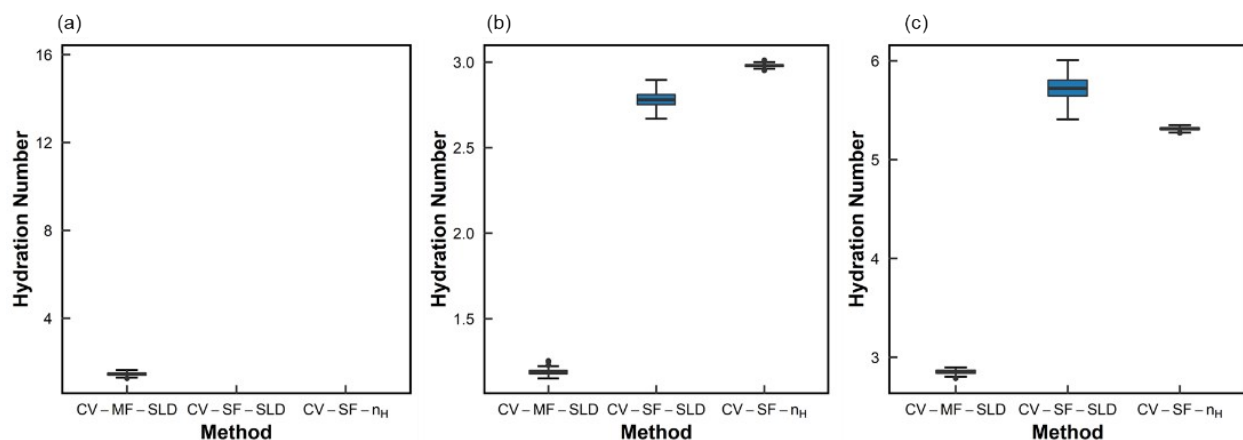


Figure S63. Box-and-whisker plots for hydration number obtained through different fitting methods for (a) PNIPAM, (b) PHPA, and (c) PDMAPS in concentrated solution (250 mg/mL). PNIPAM does not take on a Zimm structure factor in concentrated solution. Each dataset is generated from 100 bootstrapped replicates.

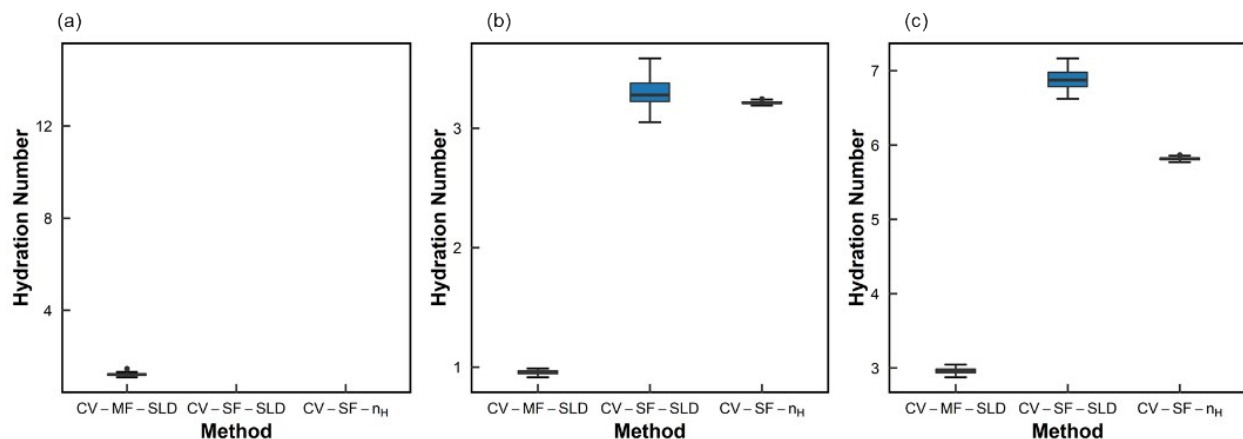


Figure S64. Box-and-whisker plots for hydration number obtained through different fitting methods for (a) PNIPAM, (b) PHPA, and (c) PDMAPS in concentrated solution (300 mg/mL). PNIPAM does not take on a Zimm structure factor in concentrated solution. Each dataset is generated from 100 bootstrapped replicates.

Table S1. Comparison of n_H from Fitting Methods in Semidilute Solution (50 mg/mL)

Pair 1	Pair 2	PNIPAM		PHPA*		PDMAPS	
		p-value	Cohen's d	p-value	Cohen's d	p-value	Cohen's d
CV-MF-SLD	CV-SF-SLD	< 0.001	-0.56			< 0.001	3.68
CV-MF-SLD	CV-SF- n_H	< 0.001	6.50	< 0.001	-13.57	< 0.001	-93.68
CV-SF-SLD	CV-SF- n_H	< 0.001	3.08			< 0.001	-25.61

*CV-SF-SLD fit for PHPA at 50 mg/mL did not converge

Table S2. Comparison of n_H from Fitting Methods in Concentrated Solution (250 mg/mL)

Pair 1	Pair 2	PNIPAM*		PHPA		PDMAPS	
		p-value	Cohen's d	p-value	Cohen's d	p-value	Cohen's d
CV-MF-SLD	CV-SF-SLD			< 0.001	-48.58	< 0.001	-31.34
CV-MF-SLD	CV-SF- n_H			< 0.001	-124.42	< 0.001	-127.26
CV-SF-SLD	CV-SF- n_H			< 0.001	-6.34	< 0.001	4.53

*PNIPAM does not have a Zimm structure factor

Table S3. Comparison of n_H from Fitting Methods in Concentrated Solution (300 mg/mL)

Pair 1	Pair 2	PNIPAM*		PHPA		PDMAPS	
		p-value	Cohen's d	p-value	Cohen's d	p-value	Cohen's d
CV-MF-SLD	CV-SF-SLD			< 0.001	-29.37	< 0.001	-44.40
CV-MF-SLD	CV-SF- n_H			< 0.001	-156.73	< 0.001	-97.49
CV-SF-SLD	CV-SF- n_H			< 0.001	1.01	< 0.001	12.41

*PNIPAM does not have a Zimm structure factor

Hydration Number in Concentrated Solution (300 mg/mL)

Table S4. Fitting Parameters for Concentrated Solution Polymers (300 mg/mL)

Polymer	Method	Rg [nm]	$Nv_p\phi(v_{ex}/V)$	v_p [nm ³]	n_H
PNIPAM	CV-MF-SLD			0.154 ± 0.002	1.22 ± 0.05
	CV-SF-SLD	4.28 ^a	not Zimm structure factor		
	CV-SF- n_H	4.28 ^a			
PHPA	CV-MF-SLD			0.1722 ± 0.0007	0.96 ± 0.02
	CV-SF-SLD	4.48 ^a	1.160 ± 0.008	0.189 ± 0.002	3.29 ± 0.1
	CV-SF- n_H	4.48 ^a	1.169 ± 0.008	0.186526 ± 1 × 10 ⁻⁶	3.214 ± 0.01
PDMAPS	CV-MF-SLD			0.354 ± 0.002	2.96 ± 0.04
	CV-SF-SLD	4.27 ^a	1.09 ± 0.01	0.357 ± 0.002	6.88 ± 0.01
	CV-SF- n_H	4.27 ^a	1.098 ± 0.007	0.339038 ± 1 × 10 ⁻⁶	5.82 ± 0.02

^a fixed from D-FF-SLD fit (for computational efficiency in linked, bootstrapped fits)
Error bars represent ± 1σ over 100 bootstrapped replicates

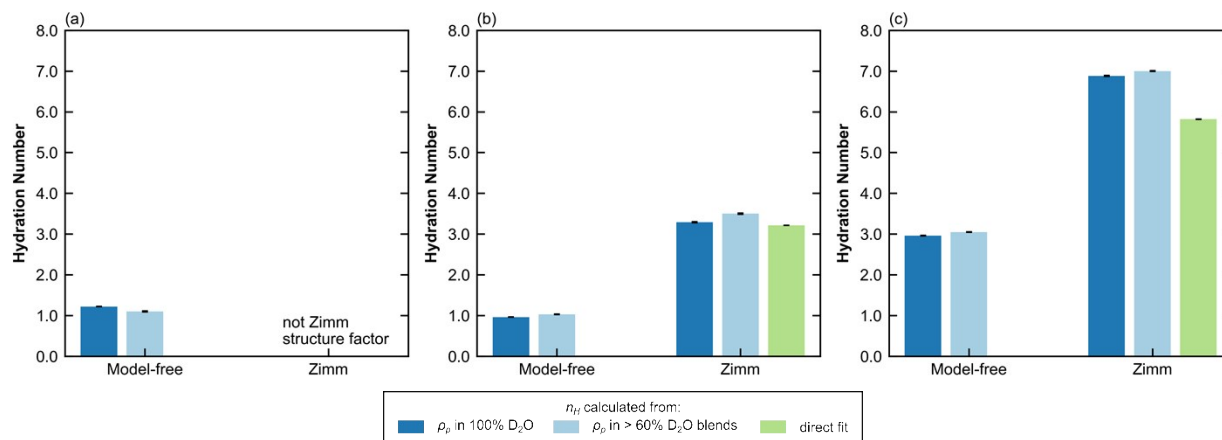


Figure S65. Bar charts comparing the hydration number obtained through different fitting methods in the concentrated regime (300 mg/mL) for (a) PNIPAM, (b) PHPA, and (c) PDMAPS. The hydration numbers obtained from SLD (dark and light blue bars) are from the CV-SANS approach (i), and directly fit hydration numbers are from approach (ii). The light blue bars represent hydration numbers averaged across high D₂O blends. Error bars represent standard error of the mean from 100 replicates.

Estimations of Blob Correlation Length

Estimates of the blob correlation length in semidilute and concentrated solution were performed using the Ornstein-Zernike structure factor⁴ (Equation S3) in SASView. A is a scaling prefactor, ξ is the correlation length corresponding to the blob size, and B is the background. These fits were performed with the same objective function shown in Equation 4. The Levenberg-Marquardt algorithm was used for the non-linear fit in SASView.

$$I(q) = \frac{A}{1 + \xi^2 q^2} + B \quad (\text{S3})$$

Fits were performed for SANS intensities collected in 100% D₂O between the q -range of 0.1 – 8 nm⁻¹ using dI as the weights and dq to smear the structure factor. Table S5 summarizes the fitting parameters and the value of the objective function at the optimum solution (F). The parameter errors are estimated from as the square root of the diagonal of the covariance matrix from the fit.

Table S5. Fitting Parameters from Ornstein-Zernike Equation

Polymer	Concentration [mg/mL]	ϕ/ϕ^*	ξ [nm]	A	B [cm ⁻¹]	F
PNIPAM	50	1.49	1.757 ± 0.005	0.772 ± 0.003	1.0961 ± 0.001 × 10 ⁻¹	43.119
PHPA	50	1.27	4.245 ± 0.01	5.19 ± 0.02	8.036 ± 0.01 × 10 ⁻²	25.715
	250	6.35	2.728 ± 0.005	7.40 ± 0.02	1.927 ± 0.002 × 10 ⁻¹	17.556
	300	7.62	2.088 ± 0.004	5.083 ± 0.01	2.313 ± 0.002 × 10 ⁻²	21.816
PDMAPS	50	0.95	4.170 ± 0.01	4.019 ± 0.01	5.516 ± 0.007 × 10 ⁻²	53.255
	250	4.76	2.684 ± 0.005	5.503 ± 0.01	1.2342 ± 0.001 × 10 ⁻¹	39.324
	300	5.71	1.949 ± 0.004	3.350 ± 0.008	1.431 ± 0.001 × 10 ⁻¹	42.079

PNIPAM Microglobule Formation

Following the approach of Yanase et al.,⁵ data for PNIPAM in concentrated solution (100% D₂O) were fit to a sum of two functions: the Ornstein-Zernike equation (OZ, first term of Equation S4) and the Lorentzian component of the pseudo-Voight equations (VL, second term of Equation S4).

$$I(q) = \frac{A_{OZ}}{1 + \xi_{OZ}^2 q^2} + \frac{A_{VL}}{1 + \xi_{VL}^2 (q - q_0)^2} + B \quad (S4)$$

These fits were implemented in SASView using a custom model consisting of the sum of two built-in functions: **lorentz** (OZ) and **peak_lorentz** (VL). The fitting algorithm and objective function are the same as described in the previous section (Estimations of Blob Correlation Length). Fitting parameters are summarized in Table S6, and fits are shown in Figure S66.

Table S6. Fitting Parameters for High Concentration PNIPAM SANS Intensities

Concentration [mg/mL]	ϕ/ϕ^*	ξ_{OZ} [nm]	A_{OZ}	q_0 [nm ⁻¹]	d_0 [nm]	ξ_{VL} [nm]	A_{VL}	B [cm ⁻¹]	F
250	7.44	3.02 ± 0.02	1.316 ± 0.007	1.685 ± 0.007	3.73 ± 0.02	1.068 ± 0.009	0.1402 ± 0.0008	3.003 ± 0.002 × 10 ⁻¹	30.929
300	8.92	3.63 ± 0.02	2.577 ± 0.01	2.041 ± 0.008	3.078 ± 0.01	0.940 ± 0.01	0.1132 ± 0.0006	3.226 ± 0.003 × 10 ⁻¹	36.63

The parameter ξ_{OZ} represents the correlation length of polymer blobs. The parameter ξ_{VL} is the inverse of the half width at half maximum of the VL function. The parameter $d_0 (= 2\pi/q_0)$ measures the correlation length between microglobules. As the concentration increases from 250 to 300 mg/mL, the average distance between microglobules decreases. However, it is important to note that the fit is imperfect, particularly in the mid- q region where a broad correlation peak or shoulder arises in the intensity curve and also in the low- q region in Figure S66b, where concentration-induced depression appears.

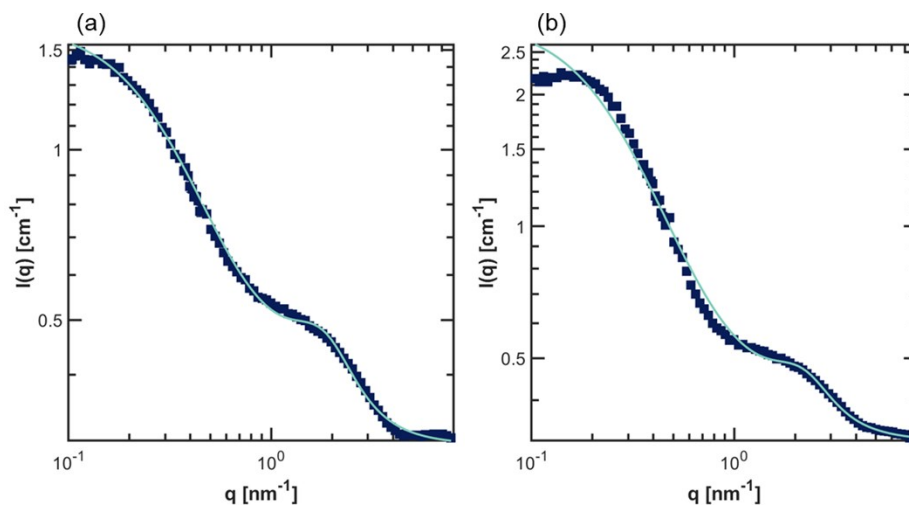


Figure S66. Fits to Equation S4 for PNIPAM in (a) 250 and (b) 300 mg/mL solutions (100% D₂O). Error bars (standard deviation from the instrument) are smaller than the data markers.

References

1. C. S. Thomas, Doctor of Philosophy in Chemical Engineering, Massachusetts Institute of Technology, 2014.
2. D. Chang, C. N. Lam, S. Tang and B. D. Olsen, *Polym Chem*, 2014, **5**, 4884-4895.
3. D. Chang and B. D. Olsen, *Polym Chem*, 2016, **7**, 2410-2418.
4. M. Rubinstein and R. H. Colby, *Polymer Physics*, Oxford University Press, New York, 2017.
5. K. Yanase, R. Buchner and T. Sato, *Phys Rev Mater*, 2018, **2**, 085601.